A multi-purpose open-source triggering platform for magnetic resonance

which was published in:
J. Magn. Reson. 247, 15–21 (2014)
doi: 10.1016/j.jmr.2014.08.009

A multi-purpose open-source triggering platform for magnetic resonance

T.Ruytenberg, A.G.Webb, and J.W.M. Beenakker

C.J.Gorter Center for High Field MRI, Department of Radiology
Leiden University Medical Center, Leiden , The Netherlands.

Corresponding author.
J.W.M. Beenakker,
C.J.Gorter Center for High Field MRI,
Department of Radiology, C3-Q
Leiden University Medical Center,
Albinusdreef 2, Leiden 2333 ZA,
The Netherlands.
Telephone: +31-71-5297381
Email: J.W.M.Beenakker@lumc.nl

Keywords: cardiac MRI, Arduino, open-source, acoustic trigger

ABSTRACT

Many MR scans need to be synchronised with external events such as the cardiac or respiratory cycles. For common physiological functions commercial trigger equipment exists, but for more experimental inputs these are not available. This paper describes the design of a multi-purpose open-source trigger platform for MR systems.

The heart of the system is an open-source Arduino Due microcontroller. This microcontroller samples an analogue input and digitally processes these data to determine the trigger. The output of the microcontroller is programmed to mimic a physiological signal which is fed into the electrocardiogram (ECG) or pulse oximeter port of MR scanner. The microcontroller is connected to a Bluetooth dongle that allows wireless monitoring and control outside the scanner room.

This device can be programmed to generate a trigger based on various types of input. As one example, this paper describes how it can be used as an acoustic cardiac triggering unit. For this, a plastic stethoscope is connected to a microphone which is used as an input for the system. This test setup was used to acquire retrospectively-triggered cardiac scans in ten volunteers. Analysis showed that this platform produces a reliable trigger (>99% triggers are correct) with a small average 8 ms variation between the exact trigger points.

INTRODUCTION

The integration of external monitoring and/or triggering equipment with MR scanners is an important component of many types of scans. For example, triggering via an MRI-compatible electrocardiogram (ECG) electrode array is required for functional cardiac scans.[1-3] Localized MR spectroscopy of the liver relies on acquiring data over repeated breathing cycles, requiring respiratory gating of the data acquisition to ensure that the signal arises from the same voxel for each signal average.[4,5] Imaging of the eye with reduced motion artifacts relies on cued-blinking approaches [6-8] which are used to trigger data acquisition. Experiments which involve in-magnet exercise to investigate the dynamics of phosphocreatine recovery require accurate triggering of data acquisition to ensure that linewidths do not vary over the duration of the experiment. For common physiological functions commercial trigger equipment exist, but for more experimental inputs these are not available. Most commercial systems offer very little flexibility for adjusting acquisition/processing parameters, which limits their usability in sub-optimal situations. A peripheral pulse unit (PPU) which consists of an MRI-compatible pulse oximeter, for example, often fails in patients with rheumatoid arthritis due to the low blood flow in their fingers. Many of these types of triggering units also face increased challenges when the magnetic field strength used for the experiment is high. It is well-known, for example, that the increased hydromagnetodynamic effect means that the ECG signal at 7 Tesla is far more difficult to trigger from than that at 1.5 Tesla or 3 Tesla[9-12], and requires additional signal filtering: even with these changes the triggering efficiency can be much lower. Temperature sensors using fibre-optics are known to have a magnetic-field dependent offset, and devices using transistor-based amplifiers often display orientation-dependent behavior due to the effects on the bias currents from the main magnetic field, Overall, then, there is a strong incentive to be able to custom design monitoring and triggering units for high field applications, with a high degree of flexibility in the design. This paper describes such a versatile open-source triggering platform for MR scanners, which gives the user the flexibility to easily integrate new physiological inputs and to adapt the signal-processing algorithm for optimal performance. The platform incorporates open-source software to allow other groups to improve and expand the performance of such devices, thus making them more available to the community-at-large. This platform therefore allows MR scientists to integrate their custom designed sensors with commercial MRI scanners.

MATERIALS

The system is designed for a Philips Achieva whole body 7T MRI system, but the setup is portable to all field strengths and commercial vendors. A schematic representation of the setup is shown in Fig.

1: details of each stage are covered in the following sections. The input signal to the setup is produced from a physiological device such as an acoustic microphone, an infra-red motion sensor, an accelerometer, or an electrode measuring an electromyelogram or electroencephalogram. The first stage of the multi-purpose trigger device is a low-pass analogue filter which removes any interference that arises from gradient switching, and provides a variable degree of amplification. The resulting signal is digitized and this signal further processed by an Arduino Due microcontroller. The microcontroller generates the required trigger outputs to, for example, the ECG or PPU port of the host computer of the MRI system. The setup is additionally equipped with a Bluetooth dongle, which allows for wireless monitoring and control outside the scanner room.

1. Input signal filtering and amplification

The first stage consists of three modules, which are shown in Fig. 2. First an operational amplifier (op-amp) adds an offset of one-half of the rail voltage (V_{CC}) to the input signal, which prevents subsequent stages from amplifying negative voltages. In addition to the desired input signal, there may be significant interference from the signal transmitted by the RF coil and switching of the magnetic field gradients during the sequence. The device is shielded from the electrical interference, caused by the RF-coil and the short switching times of the gradients (typically at several kHz), by surrounding it with a layer of thin copper. The repetitive nature of the gradient switching also results in low frequency crosstalk, both electronically and acoustically[13]. The frequency of this crosstalk is given by the inverse of the echo time (TE), e.g. a TE of 4 ms yields a first interference peak at 250 Hz. This crosstalk is removed by a 3^{th} order low-pass filter (Chebyshev type I) with a cutoff frequency of 100 Hz. A filter with different characteristics can easily be designed using software packages such as Filterlab (Microchip Technology Inc, Chandler, AZ) and could be realized using variable resistors and capacitors (varactors). The last analogue stage consists of an additional op-amp with a potentiometer, which is used as a variable gain amplifier. The potentiometer is set such that the amplified signal covers the whole dynamic range of the ADC converter and does not need to be readjusted for different subjects. The circuit is fabricated on a Printed Circuit Board (PCB), which can be plugged directly onto the Arduino microcontroller, making the setup robust and compact.

2. Microcontroller

The heart of the device is an Arduino Due microcontroller (Arduino, www.arduino.cc). The Arduino is an inexpensive multi-purpose open-source hardware platform based on Atmel microcontroller chips. The Arduino can be programmed using the C++ language and many libraries are available to

interface the device with other hardware such as sensors, liquid crystal displays (LCDs) and wireless communication modules. The open-source nature of the platform and its large user community give access to a large collection of software code, making it relatively simple to build new prototypes, even with little previous programming experience. The Arduino Due is equipped with 68 inputs/outputs and can be programmed to sample them at a periodic interval. Its 32-bit 85 MHz processor with 96 KB of memory provides enough computing power for real-time data processing. The Arduino Due supports multiple communication protocols, such as 2 USB-ports and 4 UARTs (hardware serial ports), which can be used to interface with other instruments.

The Arduino sample rate is set to be higher than the inverse of the repetition time (TR) of the MR scan, and must be at least be twice as high as the cut-off frequency of the third-order analogue low-pass filter in order to prevent aliasing. The current design has a sampling frequency of 400 Hz. After digitization the microcontroller digitally filters the signal and determines the trigger point. The current design consists of a (computational intensive) 6^{th} order infinite impulse response (IIR) filter, which needs to be tailored to the specific input. It can, for example, be used to remove a low frequency drift from the signal. IIR-filters use the previous unfiltered data, *X*, and the previous filtered data, *Y*, to calculate the filtered value using:

$$Y[n] = a_0X[n] + a_1X[n-1] + a_2X[n-2] + \cdots + a_jX[n-j] \\ -\left(b_1Y[n-1] + b_2Y[n-2] + \cdots + b_jY[n-j]\right) \quad (1)$$

The constant *j* is given by the order of the filter and the constants *a* and *b* are filter dependent and can be calculated using, for example, the scipy signal processing library in Python (scipy.org). In our design we use the Butterworth Filter function because its frequency response is flat compared to, for example, a Chebyshev filter, which has steeper transition zones but has significant ripples in its passband frequency response.

The trigger point is determined by an adaptive threshold, which is determined by calculating the standard deviation of the signal over the previous 4 seconds. These calculations require slightly less than 50% of the available computation power. The current implementation of the digital filter uses floating-point mathematics, which is about an order of magnitude slower than integer mathematics. If the code were to be rewritten to use integers, which should not significantly reduce its accuracy due to the 32 bit architecture, the required processing power will be less than 10%. This opens the possibility of more sophisticated processing algorithms such as gating or arrhythmia rejection.

3. Scanner interface

In order to make the system as independent of vendor and system architecture as possible, the output of the microprocessor is programmed to mimic a physiological signal and is fed into the corresponding physiological input of the scanner so that MR data acquisition can be triggered without requiring any software changes to the MR system itself. Initial tests have been performed by connecting the output to either the ECG- or the PPU-unit. The ECG measures a potential difference between three, or more, leads. Therefore electrical connections between the triggering unit and the ECG unit were made. The PPU, on the other hand, measures changes in light intensity, which can be mimicked by modulating a light emitting diode (LED) inside the PPU-unit. Both methods have successfully been used to generate a trigger in the MR-system. The PPU interface was preferentially chosen because of its galvanic isolation from the rest of the MR scanner. The LED is placed within the shielding of the triggering unit and the light is sent through an acrylic finger that is positioned in the PPU unit, which results in a stable trigger. A more detailed description of this interface can be found in the Appendix. The trigger detection of the MRI scanner adds an additional delay, which can be circumvented by sending the trigger directly to the scanner. This method is, however, vendor and scanner specific and is therefore not pursued in this study.

4. Data logging and wireless monitoring

The Arduino Due is equipped with four serial communication channels allowing easy interfacing with other equipment. An open-source data-logger (OpenLog, Sparkfun, CO) is connected to one of these channels. This device is programmed to save all the measured data, which greatly facilitates debugging of the setup. A second serial port is attached to a Bluetooth dongle (BlueSMiRF Gold, Sparkfun, CO) that is used for wireless monitoring and control of the microcontroller. A small hole, 5 mm x 17 mm, enables the Bluetooth signal to pass through the copper shielding. By placing a second Bluetooth dongle outside of the scanner room in front of the waveguide (which does not completely block the 2.4 GHz Bluetooth signal) wireless communication is possible between the host computer and the triggering unit. A python script is used to plot the input signal in real-time, as shown in Fig. 3B,C, and to send instructions to the microcontroller. It can, for example, override the automatic trigger level determination and set it to a fixed value based on the data that are plotted. The Bluetooth frequency is approximately eight-times higher than the proton resonance frequency at 7 Tesla, which makes the crosstalk between the MR signal and the wireless communication negligible. This is confirmed by measuring MR spectra with and without the triggering unit on the patient bed (data not shown).

5. Power supply

The whole system is powered by two 3.7V 1800 mAh Li-ion batteries (STPL-10, Conrad Electronics, Oldenzaal, NL), connected in series, which are regulated to 3.3V (V_{CC}) by the Arduino board. The whole setup uses about 100 mAh per hour, allowing it to be used for multiple sessions without recharging.

6. Acoustic cardiac triggering

The initial test project is to produce a unit for acoustic cardiac triggering (ACT) at 7 Tesla, adapting the approach of the Frauenrath *et al.*[9-12]. When a charged particle moves through a magnetic field, a small electric field is created by the Lorentz-force, the so called Hall-effect[14]. The charged particles in the blood, mainly Na^+ and Cl^-, generate such an electric field, which at high magnetic fields dominates the ECG signal[15,16]. Frauenrath *et al.* have shown that this problematic interference can be overcome with an acoustic, instead of electrical, measurement of the heart. The trigger-device is tested by connecting an electret microphone (AOM-6545P-R; Projects Unlimited, Dayton, OH) to the analogue input of the multi-purpose triggering unit and connecting this, via a flexible plastic tube (Aqua One, outer diameter 12 mm, inner diameter 9mm), to a 3D printed nylon-12 stethoscope with a silicone membrane. The stethoscope is placed on the chest of the volunteer and held in place with an adjustable elastic belt, as is shown in Fig. 3A. Low tip-angle gradient echo scans of the heart are made using retrospective gating and an eight channel transmit/receive array coil[17]. All protocols were approved by the local medical ethics committee, and informed consent was obtained from all volunteers.

Two different versions of the setup for the use as an ACT have been developed. The first design uses the previously described PCB and performs all subsequent filtering steps digitally, allowing for more flexibility. The second design uses an ACT-specific PCB, which performs all filtering in an analogue fashion. This design has less flexibility, but uses significantly less CPU power of the microcontroller which can subsequently be used for more sophisticated trigger detection.

For the first, more general, setup, the digital processing of the microprocessor is configured as a 40 Hz 6^{th}-order high-pass filter followed by a rectifier and a moving-average filter. This effectively calculates the envelope of the acoustic input, as shown in Fig. 4A. The microprocessor generates a trigger if the signal reaches the threshold value. A minimum delay of 400 ms between triggers is set to prevent false triggers on the second heart tone (typically two distinct heart tones are recorded, corresponding to different heart valves opening and closing).

The second, ACT specific, setup performs all the filtering necessary for cardiac triggering in an analogue fashion (a 4th order band-pass with a lower 40 Hz and upper 100 Hz cut-off, followed by a rectifier). The microprocessor is used to generate a trigger if the input is above the threshold in a similar way as with the general design.

RESULTS

With the acoustic cardiac triggering setup ten healthy volunteers (5 male, 5 female) have successfully been scanned using both ACT designs. During scanning the filtered acoustic signal with the trigger point was monitored real-time. Most of the cardiac scans were acquired during a 12s expiratory breath-hold. The deep inhalations that the volunteers make before the actual scan, have a much higher sound intensity than during the breath hold, as is shown in Fig. 4C. This is most likely the result of different acoustic properties of the abdomen and thorax during deep inhalation. This effect leads to an unstable threshold calculation by the adaptive threshold algorithm. The threshold was therefore set to a fixed value prior to such a scan using the monitoring software.

Real-time plotting of the acoustic signal, shown in Fig. 3B, is very useful in determining the optimal position of the stethoscope. The acoustic signal proved to be strong enough that the volunteer could still wear a surgical gown below the stethoscope, which increases patient privacy and comfort.

The microcontroller generated correct triggers in >99% of the heartbeats, Fig. 5C, with both the more general and ACT-specific version of the PCB and corresponding software. None of the scans from any of the ten volunteers showed any visible motion artefacts which would occur if there were errors in the trigger signal. Figure 5AB show a four-chamber and short axis scan taken from two of the volunteers.

Comparison of acoustic and electrical cardiac signals

The accuracy of the triggering device was tested by simultaneously measuring an electrocardiogram (ECG) and the acoustic heart signal outside the magnet. Most commercial ECG units do not have the possibility to output the ECG signal real time, and since this would hinder the determination of the exact trigger delay, a small ECG-circuit was built. A description of this setup can be found in the Appendix. The setup was used to measure 317 heartbeats. Visual inspection of the data showed no missed heartbeats for all three inputs.

The comparison between the ACT and the ECG triggers, Fig. 6, shows a trigger delay of approximately 60 ms between the R-peak of the ECG and the acoustic based triggers. During the measurement, the volunteer spoke on three occasions. This resulted in an additional acoustic signal causing a too early trigger. On several occasions, the intensity of the acoustic signal was temporarily lower, which led to an increased delay of approximately 75 ms.

A statistical comparison of the trigger delays, excluding the three triggers caused by the volunteer speaking, show similar results for both designs. For the dedicated ACT PCB the trigger delay is partly due to the approximately 20 ms group delay of the band-pass filter. The time between onset of the acoustic signal and the trigger threshold is on average 30 ms. Lowering the trigger threshold could decrease this delay, but would to lead to some false triggers. The 2 m-long acoustic wave-guide, between the stethoscope and the microphone, adds another 6 ms delay. The ECG-signal, measured during an MR scan, needs to be filtered in order to remove the gradient and RF interference. An analogue filter to remove this interference would add a delay of at least 15 ms, whereas the peak detection algorithm would add another few milliseconds. This will make the delay between a MR compatible ECG and the acoustic trigger device approximate 35 ms.

The trigger jitter, the variation in trigger delay measured as the standard deviation of the trigger delay, is an important measure for the reliability of the trigger detection. A large trigger jitter would result in motion artefacts in the MR images. The trigger jitter of the setup is approximately 8 ms and is similar to the repetition time of the MR scan. Therefore no additional synchronisation errors are generated by the use of the multi-purpose trigger device.

DISCUSSION

This setup is able to reproducibly (>99%) deliver triggers to the MR scanner based on a custom analogue input. Besides retrospectively-triggered cardiac MRI scans, this setup has also successfully been used for prospectively-triggered diffusion weighted MR spectroscopy measurements of the brain (data not shown). The design of an application specific PCB, which performs all signal filtering in an analogue fashion, results in both situations in a slightly more reproducible trigger. The low frequency acoustic interference, mainly caused by breathing, is at least an order of magnitude greater than the acoustic cardiac signal. The greatest benefit of the dedicated filter design is that this interference is removed before the signal is amplified and subsequently digitized. The dedicated filter therefore allows a higher amplification setting to be used, which would otherwise have resulted in

clipping, and thus provides an increased signal intensity. This makes the positioning of the stethoscope, for example, less critical, because even a sub-optimally positioned stethoscope still yields sufficient signal. Another advantage of a dedicated analogue filter is that the microprocessor time can be used to detect incorrect triggers. It can, for example, be programmed to send a reject-last-trigger signal to the MR if the signal peak height is not within a specific range.
The versatility of the Arduino platform allows this setup to generate triggers based on various types of input. The many inputs and outputs of the Ardunio, together with the wireless communication, furthermore allow this device to be used to remotely monitor and control equipment inside the scanner room.

AVAILABLE RESOURCES

To facilitate the further development of this platform, and in accordance with the Arduino philosophy, the design of the setup, together with the used Arduino and python scripts, are available open source. Please contact the author at: j.w.m.beenakker@lumc.nl

ACKNOWLEDGEMENTS

The authors thank W.M. Brink for assistance with the cardiac MRI scans.

APPENDIX

Interface to the MRI scanner using the PPU unit

The physiological pulse-oximeter signal is simulated using a LED. The LED is placed within the shielding of the triggering unit and the light is sent through an acrylic finger that is positioned in the PPU unit. The PPU-hardware filters the signal in such a way, that a simple blinking LED results in unstable trigger detection by the MR software. By adding a small compensatory section after every trigger, as is shown in Fig. 7, a stable trigger detection is achieved.

ECG design

The MR scanner used for these experiments is equipped with both an ECG input and a PPU input, but does not allow both inputs to be used simultaneously. The commercial ECG units available to us did not have an appropriate real-time output, which prevented a good comparison with the triggering unit. We therefor build a simple ECG amplifier, described below, as this guarantees no unwanted delays in the ECG signal and therefore allows for a valid comparison with the triggering unit.
Three ECG-electrodes (Cleartrace2, ConMed Corp. Utica, NY) were attached to the subjects right arm (RA), left leg (LL) and right leg (RL). The setup is configured in lead II configuration, meaning the RA and LL are connected to the inputs of the instrumental amplifier (AD620, Analog Devices, Norwood, MA) and RL is connected to ground, as is shown in Fig. 8. The instrumental amplifier amplifies the difference between the input signals by a factor of 248 (this is set by the 200 Ohm resistor) and the output is high-pass filtered (cut-off frequency 0.03 Hz) to remove the DC offset. To ensure safety a diode pair is placed between the inputs of the ECG, and a current-limiting power supply is used. The output of the ECG, together with the outputs of both the general and dedicated ACT PCB are connected to the analogue inputs of the Arduino.

The Arduino is programmed to sample the three channels at 800 samples/second and stores the data on an SD card without any further processing. A python script analyses the acoustic data with the same algorithm normally used on the Arduino to generate the triggers. The R-peaks in the ECG signal are detected by a simple peak-finding algorithm and selecting only the peaks above a user defined threshold. All three algorithms successfully detected 317 heartbeats. Visual inspection of the data showed no missed heartbeats.

REFERENCES

[1] P. Lanzer, E.H. Botvinick, N.B. Schiller, L.E. Crooks, M. Arakawa, L. Kaufman, et al., Cardiac imaging using gated magnetic resonance, Radiology. 150 (1984) 121–127. doi:10.1148/radiology.150.1.6227934.

[2] D. Buikman, T. Helzel, P. Röschmann, The rf coil as a sensitive motion detector for magnetic resonance imaging, Magnetic Resonance Imaging. 6 (1988) 281–289. doi:10.1016/0730-725X(88)90403-1.

[3] J.M. Rubin, J. Brian Fowlkes, M.R. Prince, R.T. Rhee, T.L. Chenevert, Doppler US gating of cardiac MR imaging, Academic Radiology. 7 (2000) 1116–1122. doi:10.1016/S1076-6332(00)80065-3.

[4] A. Qayyum, MR Spectroscopy of the Liver: Principles and Clinical Applications1, Radiographics. 29 (2009) 1653–1664. doi:10.1148/rg.296095520.

[5] S.M. Noworolski, P.C. Tien, R. Merriman, D.B. Vigneron, A. Qayyum, Respiratory motion-corrected proton magnetic resonance spectroscopy of the liver, Magnetic Resonance Imaging. 27 (2009) 570–576. doi:10.1016/j.mri.2008.08.008.

[6] B. Berkowitz, M. Detroit, D. Canfield, C. McDonald, Y. Ito, P. Tofts, et al., Measuring the human retinal oxygenation response to a hyperoxic challenge using MRI: Eliminating blinking artifacts and demonstrating proof of concept, Magnetic Resonance in Medicine. 46 (2001) 412–416. doi:10.1002/mrm.1206.

[7] J.W.M. Beenakker, G.A. van Rijn, G.P.M. Luyten, A.G. Webb, High-resolution MRI of uveal melanoma using a microcoil phased array at 7 T, NMR Biomed. 26 (2013) 1864–1869. doi:10.1002/nbm.3041.

[8] T. Lindner, S. Langner, A. Graessl, J. Rieger, M. Schwerter, M. Muhle, et al., High spatial resolution in vivo magnetic resonance imaging of the human eye, orbit, nervus opticus and optic nerve sheath at 7.0 Tesla, Exp. Eye Res. 125C (2014) 89–94. doi:10.1016/j.exer.2014.05.017.

[9] T. Frauenrath, F. Hezel, U. Heinrichs, S. Kozerke, J.F. Utting, M. Kob, et al., Feasibility of Cardiac Gating Free of Interference With Electro-Magnetic Fields at 1.5 Tesla, 3.0 Tesla and 7.0 Tesla Using an MR-Stethoscope, Investigative Radiology. 44 (2009) 539–547. doi:10.1097/RLI.0b013e3181b4c15e.

[10] M. Becker, T. Frauenrath, F. Hezel, G.A. Krombach, U. Kremer, B. Koppers, et al., Comparison of left ventricular function assessment using phonocardiogram- and electrocardiogram-triggered 2D SSFP CINE MR imaging at 1.5 T and 3.0 T, Eur Radiol. 20 (2010) 1344–1355. doi:10.1007/s00330-009-1676-z.

[11] T. Frauenrath, T. Niendorf, M. Kob, Acoustic Method for Synchronization of Magnetic Resonance Imaging (MRI), Acta Acustica United with Acustica. 94 (2008) 148–155. doi:10.3813/AAA.918017.

[12] T. Frauenrath, F. Hezel, W. Renz, T. d'Orth, M. Dieringer, F. von Knobelsdorff-Brenkenhoff, et al., Acoustic cardiac triggering: a practical solution for synchronization and gating of cardiovascular magnetic resonance at 7 Tesla, J Cardiovasc Magn Reson. 12 (2010) 67. doi:10.1186/1532-429X-12-67.

[13] R.A. Hedeen, W.A. Edelstein, Characterization and prediction of gradient acoustic noise in MR imagers, Magnetic Resonance in Medicine. 37 (1997) 7–10. doi:10.1002/mrm.1910370103.

[14] E.H. Hall, On a New Action of the Magnet on Electric Currents, American Journal of Mathematics. 2 (1879) 287. doi:10.2307/2369245.

[15] R.R. Price, The AAPM/RSNA physics tutorial for residents. MR imaging safety considerations. Radiological Society of North America, Radiographics. 19 (1999) 1641–1651. doi:10.1148/radiographics.19.6.g99no331641.

[16] A. Gupta, A.R. Weeks, S.M. Richie, Simulation of Elevated T-Waves of an ECG Inside a

Static Magnetic Field (MRI), Biomedical Engineering, IEEE Transactions on. 55 (2008) 1890–1896. doi:10.1109/TBME.2008.919868.

[17] A. Raaijmakers, I. Voogt, D. Klomp, P. Luijten, N. van den Berg, Dipole antenna without ceramic substrate and still low SAR: the fractionated dipole antenna, in: Proc Annu Meeting ISMRM, n.d.: p. 4382.

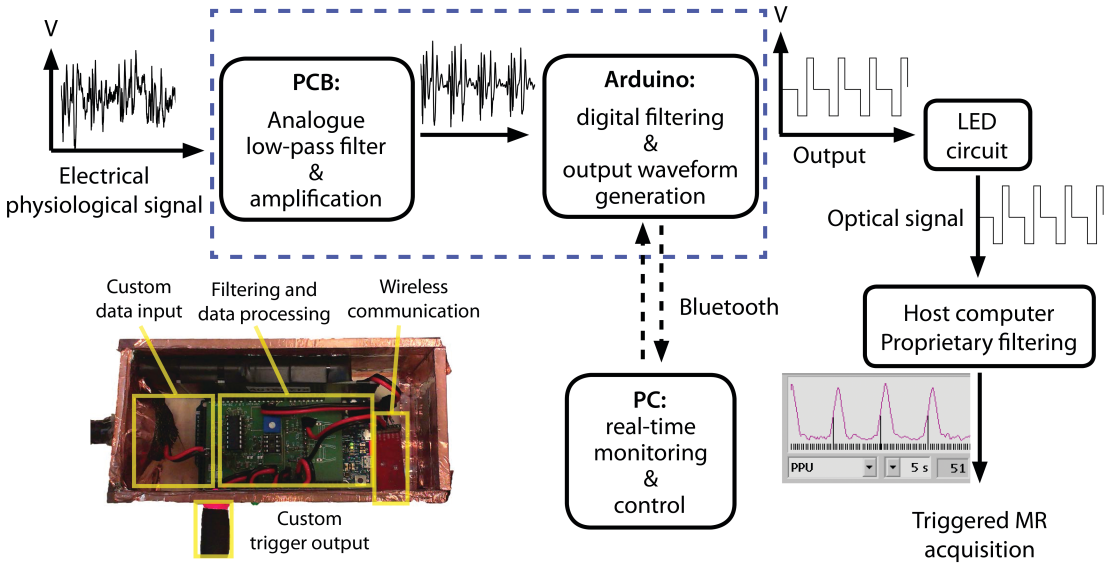

Figures

Figure 1: Schematic representation of the trigger unit. A custom analogue signal is low-pass filtered on a PCB to remove any possible gradient interference. The resulting signal is digitized and processed by an Arduino Due microcontroller, which can output a trigger signal to the ECG or PPU unit of the MRI. A Bluetooth dongle allows for wireless monitoring and control of the microcontroller. The inset shows the setup in its copper shielding.

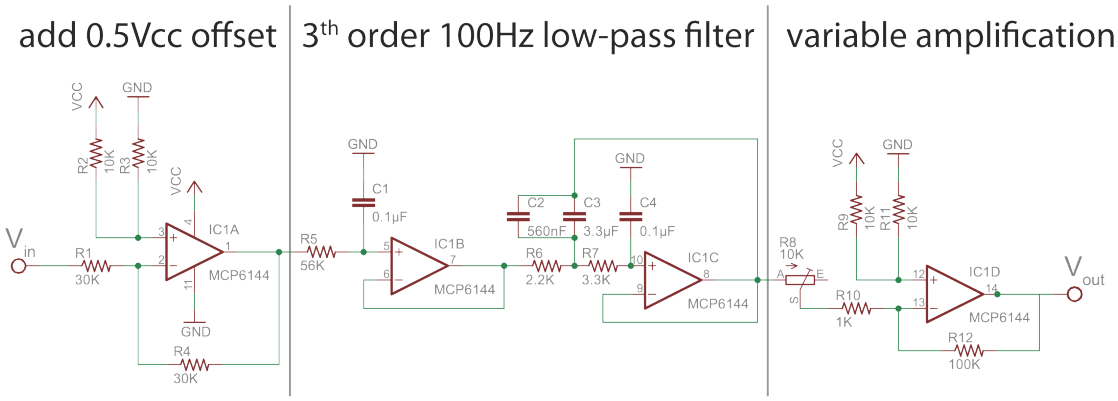

Figure 2: Schematic of the analogue filter circuit on the PBC. The first stage gives the input signal (V_{in}) an offset of $0.5V_{cc}$. The second stage is a 3th order Chebyshev type 1 filter. The characteristics of the filter can easily be changed by replacing the capacitors and resistors with different values. The last stage amplifies the signal. The amount of amplification can be adjusted by turning R8, a variable resistor. All four op-amps are combined in one component (MCP6144, Microchip, Chandler, AZ) to save space.

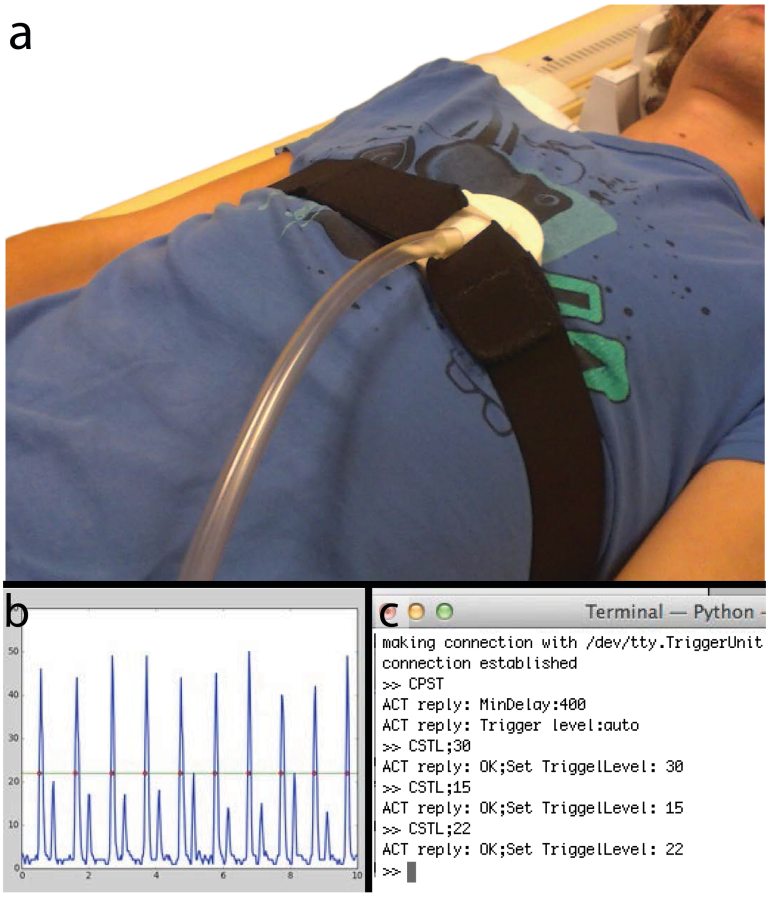

Figure 3: (A) The acoustic cardiac triggering unit consists of a shielded box with the microcontroller and a stethoscope. The stethoscope is placed on the volunteer with an adjustable elastic belt. (B) Using wireless communication, the acoustic input and the generated triggers can be monitored real-time. This greatly simplifies the positioning of the stethoscope. (C) The same Bluetooth connection is also used to remotely configure the triggering unit.

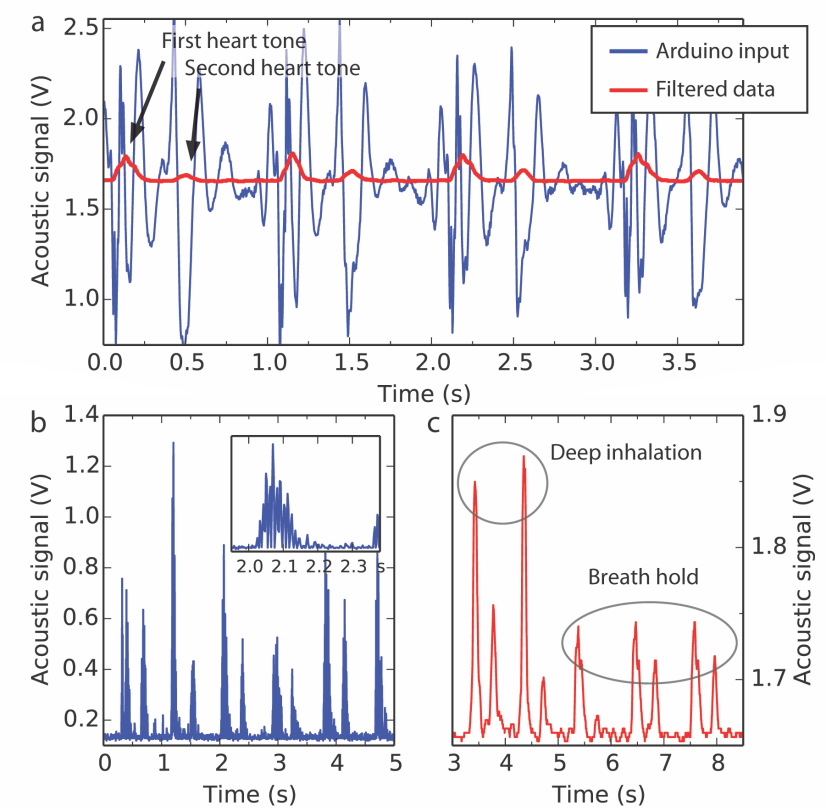

Figure 4: Digital filtering by the microcontroller of the acoustic cardiac signal.

(A) After digital filtering (a 40 Hz 6th-order high-pass IIR filter followed by a rectifier and a 30 point moving-average) the first and second heart beat can clearly be distinguished. Digital filtering leads to an additional signal delay.

(B) Output of the dedicated acoustic cardiac triggering PCB (4th order 40 and 100 Hz band-pass filter, rectified with diode). The lack of a negative power supply in the design results in a 0.13 V offset. (B inset) A zoom-in reveals the fast oscillations caused by the acoustic origin of the signal. The oscillations do not influence the trigger detection.

(C) Most cardiac scans are made during an expiratory breath hold. The deep inhalations, which are made before the breath hold, have significant higher sound intensity compared to the expiratory state, which hinders an automatic trigger level determination.

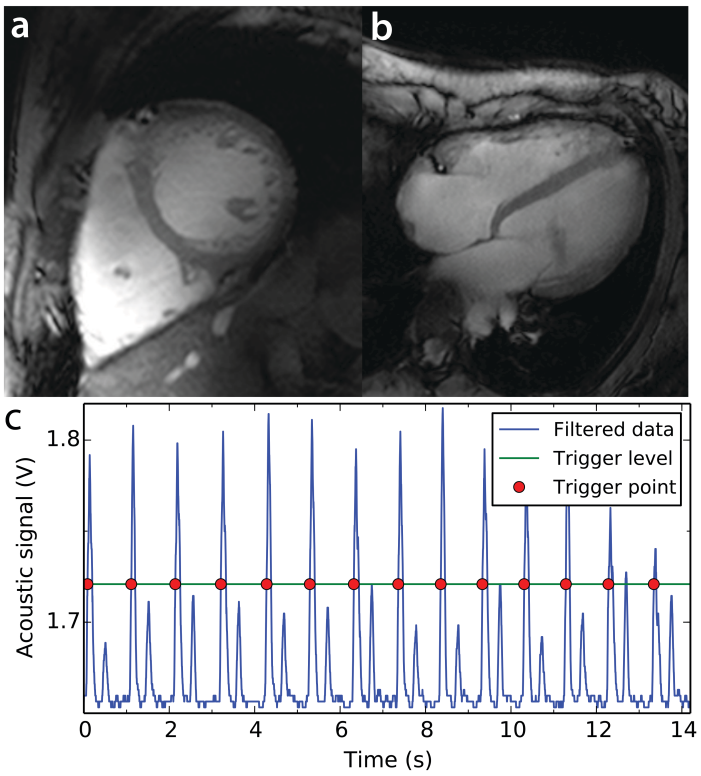

Figure 5: The acoustic triggering device has been used to acquire cardiac scans of ten different volunteers. (A) Short-axis and (B) four-chamber scan using low tip-angele gradient echos with retrospective gating (A: TR/TE/flip angle: 4.3ms/2.7ms/ 8.5°; TFE factor 12; heart phases33; 9 slices, field-of-view (FOV): 300x263x72 mm^3, spatial resolution: 1.4 x 1.4 x 8mm^3, scan time: 1min 48sec; B: TR/TE/flip angle: 4.23ms/ 2.6ms,/8.5°; Turbo Field Echo (TFE) factor 12; heart phases 33; FOV: 280x350 mm^2, spatial resolution: 1.3x 1.3x 8 mm^3, scan time: 16s).(C) The trigger device generated correct triggers in >99% of the heartbeats.

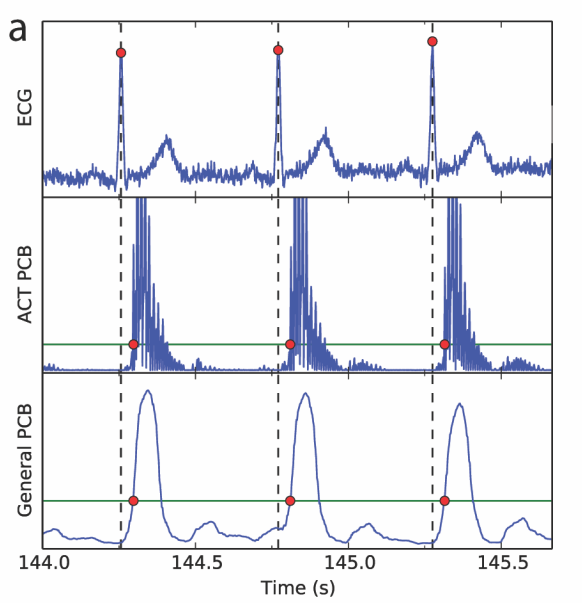

b	Trigger delay	Trigger jitter
ACT specific design	41.4 ms	4.7 ms
General design	44.6 ms	6.0 ms

Figure 6: Comparison of the ACT with an ECG

(A) The Arduino samples simultaneously the ECG signal and the output of the general PCB and the ACT specific PCB. A python script is used to detect the trigger points and successfully detected 317 heartbeats.

(B) Trigger delay statistics for the 317 heartbeats, excluding the three incorrect triggers due to the subject speaking, show an average trigger delay in the order of 60 ms with a variation of approximately 8 ms.

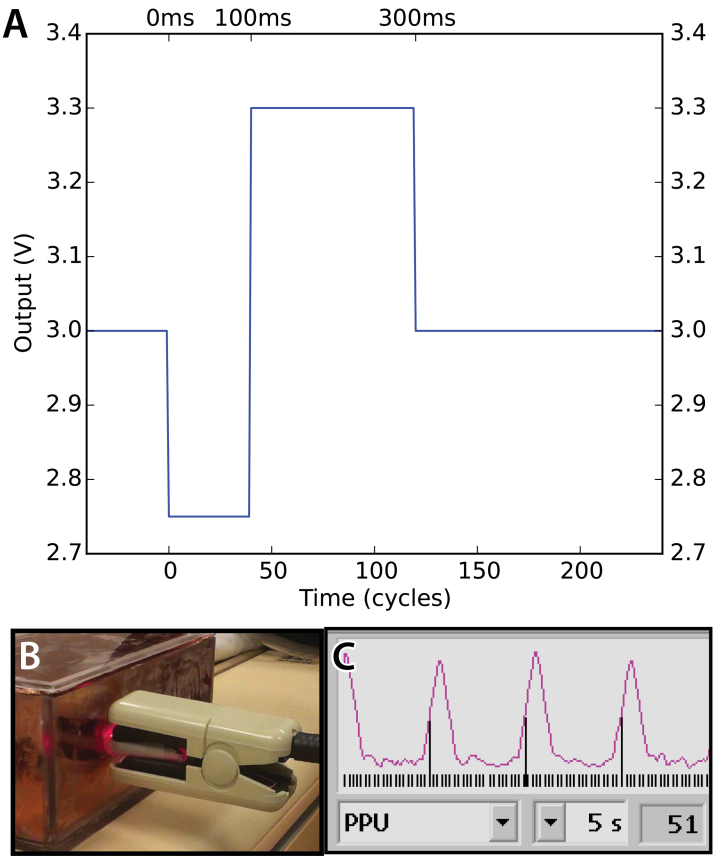

Figure 7: Interface with the MRI scanner. (A)The trigger is sent to the MRI by mimicking a pulse oximeter signal with a red LED (211-2111, Farnell, Utrecht, NL) connect in series with a 56 Ohm resistor connected to ground. The resulting current is approximately 20 mA, which corresponds to a luminosity of 400 mcd. (B) The LED illuminates through an acrylic finger, which is placed in the PPU unit. A trigger is generated by slightly dimming the LED for 100 ms. After each trigger the LED intensity is slightly increased for 200 ms to prevent the PPU hardware from changing its detection gain. (C) The resulting stable trigger detection during a cardiac triggered scan.

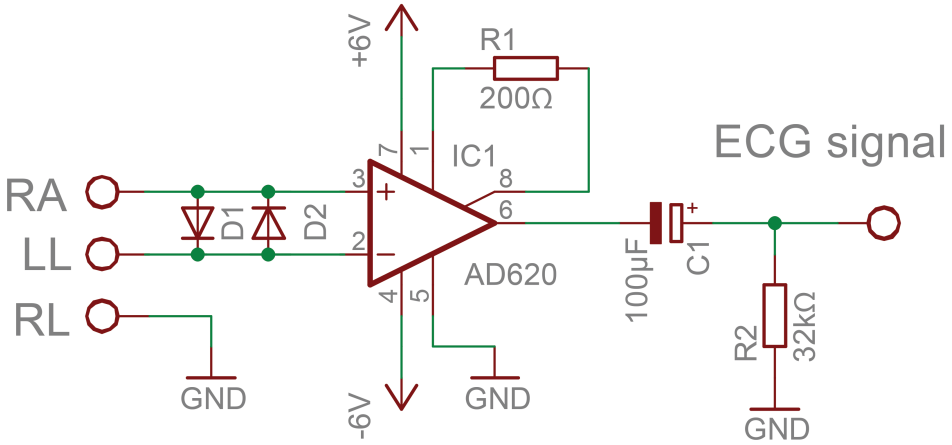

Figure 8: An ECG signal is generated by measuring the difference between a lead connected to the right arm (RA) and the left leg (LL) of a volunteer, using an instrumentation amplifier. The output of the amplifier is high-pass filtered to remove the DC offset. As a safety measure, a diode pair is placed between the inputs, which become conducting if there is more than 1V between leads. For added safety two extra diode pairs could be placed between the two inputs and the ground lead connected to the right leg (RL).